

High birefringence and high nonlinear octagonal photonic crystal fiber with low confinement loss

Mayilamu·Musideke, Yao Jianquan, Lu Ying, Wu Baoqun, Hao Congjing, Duan Liangcheng

(1. Institute of Laser & Optoelectronics, College of Precision and Opto-Electronic Engineering, Tianjin University, Tianjin, 300072, China; 2. Key Laboratory of Opto-electronics Information and Technical Science (Ministry of Education), Tianjin University, Tianjin, 300072, China)

Abstract: A novel octagonal photonic crystal fiber (PCF) was designed using an elliptical air hole and large circular air hole in the core region in order to enhance the performance of modal nonlinearity, birefringence and to get the low confinement loss at the same time. Its effective mode area, nonlinearity, birefringence and confinement loss were investigated simultaneously by using finite element method(FEM) with anisotropic perfectly matched layers. The numerical simulation results show that by choosing suitable relative structure parameters that the proposed fiber has high birefringence up to the order of 1.68×10^{-2} at wavelength $1.55 \mu\text{m}$, it is about two orders of magnitude higher than that of the regular polarization maintaining fiber. High nonlinearity $\gamma=60 \text{ W}^{-1}\text{km}^{-1}$, and low confinement loss 0.6 dB/km at wavelength $1.55 \mu\text{m}$. This highly birefringence PCFs with high nonlinear coefficient have received growing attention in telecommunication, various polarization sensitive devices and supercontinuum applications systems.

Key words: photonic crystal fiber; high birefringence; high nonlinearity; low confinement loss; finite element method

CLC number: TN929.11 **Document code:** A **Article ID:** 1007-2276(2013)12-3373-07

高双折射高非线性低损耗八边形光子晶体光纤特性

马依拉木·木斯得克, 姚建铨, 陆颖, 吴宝群, 郝丛静, 段亮成

(1. 天津大学精仪学院 天津大学激光与光电子研究所, 天津 300072;
2. 光电信息技术科学教育部重点实验室, 天津 300072)

摘要: 为了同时实现高双折射高非线性并得到低损耗, 设计一种在光纤纤芯附近引入椭圆形空气孔和圆形空气孔组成的新型优化的八边形光子晶体光纤。采用全矢量有限元法结合各向异性完美匹配层, 对该光纤的有效面积、非线性、双折射和损耗特性进行了模拟分析。数值模拟结果表明, 通过选择适当的结构参数, 在波长 $1.55 \mu\text{m}$ 处, 该光纤具有高双折射高达 $B=1.68 \times 10^{-2}$, 比普通光纤高两个数量级, 高非线性系数为 $\gamma=60 \text{ W}^{-1}\text{km}^{-1}$ 和低损为 0.6 dB/km 。这种具有高双折射高非线性系数的光纤可用于光通信、偏振敏感的各种设备和产生超连续谱等领域。

关键词: 光子晶体光纤; 高双折射; 高非线性; 低损耗; 有限元法

收稿日期: 2013-03-07; 修订日期: 2013-04-12

基金项目: 国家 973 计划(2010CB327801)

作者简介: 马依拉木·木斯得克(1983-), 女, 博士, 主要从事激光器与光子晶体光纤传感器研究。Email:mahiralaser@163.com

导师简介: 姚建铨(1937-), 男, 中国科学院院士, 博士生导师, 主要从事光电子方面研究。Email:jyao@tju.edu.cn

0 Introduction

Photonic crystal fiber (PCFs) have attracted much attention due to their unique properties such as endlessly single-mode operation, chromatic dispersion management, large mode areas (LMA), high birefringence, high nonlinearity and low confinement loss^[1-5] which are not obtainable using conventional step index fibers. In recent years, growing interest has been shown in reducing the polarization coupling which is possible with birefringent PCFs. Birefringence PCFs can be realized by making the core of the PCF asymmetric. Hence, the effective index difference between the two orthogonal polarization modes increases. PCFs with six-fold rotational symmetry have zero birefringence^[6-7]. However by altering their hole size^[8] or distorting the shape of their hole (elliptical air holes)^[9] around the PCF core, six-fold rotational symmetry of the PCF is destroyed. Previously proposed PCF with elliptical air holes^[10] has demonstrated that large birefringence in the order of 10^{-3} – 10^{-2} can be achieved. Nevertheless, highly nonlinear coefficient PCFs with high birefringent have received growing attention in telecommunication and supercontinuum applications^[8,11-14]. On the other hand, PCFs based SC light sources at 1.55 μm band have become an alternative to narrow band sources used in telecommunication window such as a spectral slicing optical pulse source used in wavelength division multiplexing.

Previously, several designs for the PCFs have been proposed to achieve a high birefringence and highly nonlinear coefficient in a PCF at wavelength 1.55 μm . PCF designs are those that have modified hexagonal PCFs^[8,15-20], square PCFs^[21-23], and octagonal PCFs^[24-26]. This kind of design has not better high nonlinear coefficient and high birefringence compared with our design PCF.

In our study, we propose a PCF design that simultaneously exhibits much better performance in terms of birefringence and nonlinearity than any previously published results. Additionally, the proposed PCF has shown some interesting results in terms of low confinement loss. In order to fully investigate the key propagation characteristics of our proposed design, finite element method (FEM) has been employed. As a part of the ongoing efforts to design HB–HN–OPCF with low confinement loss, a novel five-ring OPCFs structure is proposed for the telecommunication window. Numerical simulation results show that the HB–HN–OPCF have $B=1.68 \times 10^{-2}$, nonlinear coefficients greater than $\gamma=60 \text{ W}^{-1}\text{km}^{-1}$, at 1.55 μm , and confinement loss lower than 0.6 dB/km in the same wavelength. Due to the above mentioned properties, the proposed OPCFs in this letter have many optical applications in future.

1 Structure of the OPCF and simulation method

The motivation of this study is to design OPCF structures that achieve high nonlinear coefficient, high birefringence and low losses simultaneously. Fig.1 illustrates the schematic section of the OPCF. It is the proposed structure made of regular circular and ellipse air-holes with an index-guiding core surrounded by an isosceles triangular unit lattice of a vertex angle of 45° ^[27], where the core is formed by omission of one air hole and the cladding is formed by five air hole rings, and background material such as silica glass ($n=1.45$). The hole pitch length (the center to center spacing between the air holes) is Λ , the circular air-hole diameter on the first ring is d_1 , while the air-hole diameter on the other rings is d_2 , elliptical air-holes with elliptical ratio $\eta_1=a_1/b_1$ arranged along x -axis and elliptical ratio $\eta_2=a_2/b_2$ arranged along y -axis near the core region of the

proposed design.

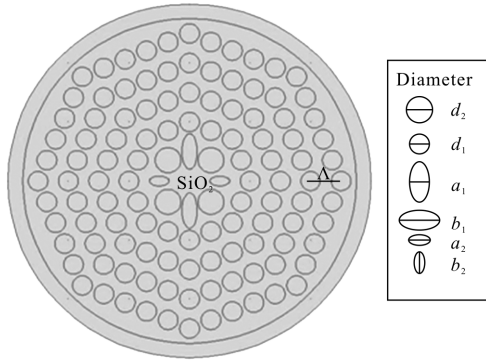


Fig.1 Cross-section of the HB-HN-OPCF

To analyze optical properties, we use the widely accepted numerical analysis method, finite element method, which provides a well-proven reliability. Using the FEM, the PCF cross-section, with the finite number of air holes is divided into homogeneous subspaces where Maxwell's equations are solved by accounting for the adjacent subspaces. These subspaces are triangles that allow a good approximation of the circular structures. Using the anisotropic PML, from Maxwell's curl equations the following vectorial equation is obtained [28–29]:

$$\nabla \times (\mu_r^{-1} \nabla \times E) - k_0^2 \epsilon_r E = 0 \quad (1)$$

Where E is the electric field vector, k_0 ($=2\pi/\lambda$) is the wave-number in the vacuum, ϵ_r and μ_r is the relative permittivity and relative permeability, respectively.

The nonlinearity coefficient $\gamma(\lambda)$ of the PCF can be defined as [30]

$$\gamma(\lambda) = \frac{n_2 \omega_0}{c A_{\text{eff}}} = \frac{\pi}{\lambda} \frac{n_2}{A_{\text{eff}}} \quad (2)$$

Where λ is the wavelength, n_2 is the fiber nonlinear refractive index, and A_{eff} is the effective mode area, which is calculated by [30]

$$A_{\text{eff}} = \frac{(\iint_s |E|^2 dx dy)^2}{\iint_s |E|^4 dx dy} \quad (3)$$

The polarization beat length L_B is a measure of the birefringence and is defined as [4]

$$L_B = \frac{2\pi}{\beta_x - \beta_y} = \frac{\lambda}{n_x - n_y} \quad (4)$$

Where β_x and β_y are the propagation constants of the two modes n_x and n_y , and are the refractive index that each mode sees, with shorter L_B corresponding to stronger birefringence. So the birefringence is expressed as [4]

$$B = |n_{\text{eff}x} - n_{\text{eff}y}| \quad (5)$$

In PCFs, the light is trapped by an enclosure of air holes and loss arises from small amounts of power leakage between and through the holes. This is termed confinement loss, which is defined by [5]

$$L_c = \frac{40\pi}{\ln(10)\lambda} \text{Im}[n_{\text{eff}}] = 8.686k_0 \text{Im}[n_{\text{eff}}] \quad (6)$$

Where $\text{Im}[n_{\text{eff}}]$ is the imaginary part of the n_{eff} .

2 Simulation results and discussion

Numerical results of the effective mode area depicted in Fig.2 under the different structures of the proposed OPCF. As may be seen from the figure, effective mode area of the fundamental mode shows different behavior for different structures. The results shown that, the effective mode area of the optical fiber basically appears the linear trend with the increasing of wavelength. When the air-filling fraction $d_1/\Lambda = d_2/\Lambda = 0.65$, $\Lambda = 1 \mu\text{m}$, $\eta_1 = 2$ are constant, while changing η_2 ranging from 2 to 2.4. It can be seen from Fig.2(a) that the A_{eff} reduces $\lambda < 1.35 \mu\text{m}$ with η_2 increasing, and $\lambda > 1.35 \mu\text{m}$ increasing with η_2 increasing. At wavelength $1.55 \mu\text{m}$ is $2.52 \mu\text{m}^2$. In addition, in Fig.2(b) shows the effective mode area of the proposed OPCF steadily decreases when the air-filling fraction $d_1/\Lambda = 0.65$, $\Lambda = 1 \mu\text{m}$, $\eta_1 = 2$ and $\eta_2 = 2.4$ are constant, while the air-hole diameter d_2 ranging from 0.65 to 0.85 with the entire wavelength range. At the same time we can see that the A_{eff} at wavelength $1.55 \mu\text{m}$ reaches $2.16 \mu\text{m}^2$. From the result we can know, d_2 effective more about the A_{eff} than the η_2 .

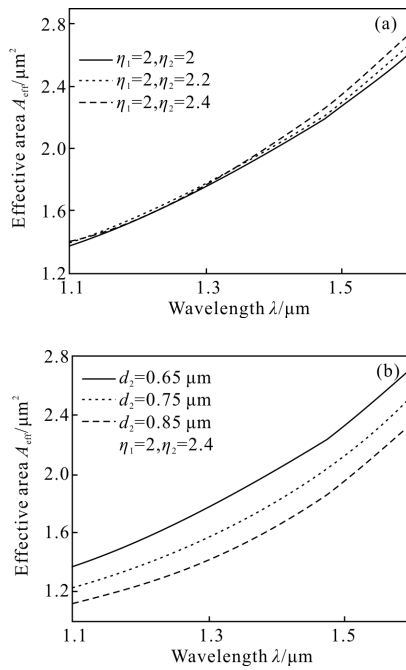


Fig.2 Nonlinear coefficient versus wavelength of the structure for changes η_2 and d_2

Then, considering the influence of different parameters on the nonlinearity coefficient are simulated and shown in Fig.3, by remaining the air filling fraction $d_1/\Lambda=d_2/\Lambda=0.65$, $\Lambda=1\ \mu\text{m}$, $\eta_1=2$, while changing η_2 from 2 to 2.4. It can be shown in Fig.3 (a) that the nonlinear coefficient is decreased with the increase of wavelength, and nonlinear coefficient is a gently dipping trend when η_2 is increased. While at wavelength $1.55\ \mu\text{m}$ we obtained smaller nonlinear coefficient $\gamma=51.3\ \text{W}^{-1}\text{km}^{-1}$. Fig.3 (b) shows that when the air filling fraction $d_1/\Lambda=0.65$, $\eta_1=2$ and $\eta_2=2.4$ are constant, and d_2 changing from 0.65 to 0.85. The nonlinear coefficient curves are almost parallel to each other. When d_2 is enlarged, the curve of nonlinear coefficient is up-shift and the value of nonlinear coefficient is increased. Adjusted the air-hole diameter d_2 to 0.85, we obtained at wavelength $1.55\ \mu\text{m}$ a larger nonlinear coefficient $\gamma=60\ \text{W}^{-1}\text{km}^{-1}$. From the result it can be seen that in order to get a large nonlinear coefficient the d_2 play an important role than η_2 .

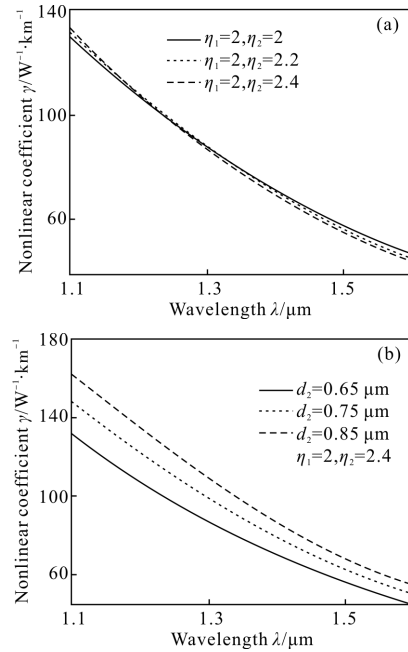


Fig.3 Nonlinear coefficient against wavelength of the structure for changes η_2 and d_2

Fig.4 illustrates the birefringence and beat length of the OPCF for $d_1/\Lambda=d_2/\Lambda=0.65$, $\Lambda=1\ \mu\text{m}$, $\eta_1=2$ and η_2 ranging from 2 to 2.4. It can be seen from Fig.4(a) that the modulus of the birefringence sharply increases with the increases of wavelength and the

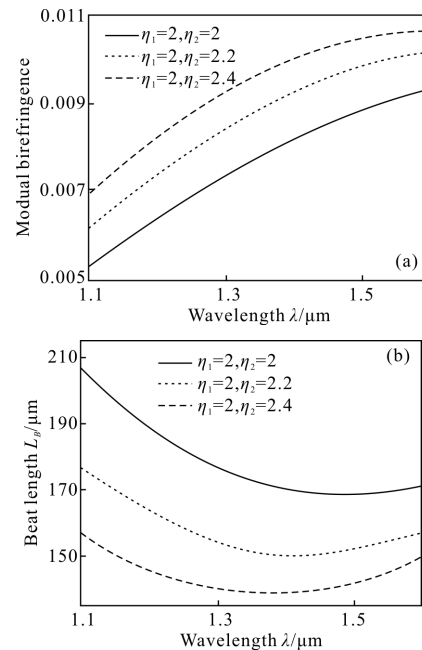


Fig.4 Birefringence and beat length of the structure for changes η_2

elliptical ratio η_2 . These parameters give a value of birefringence 1.06×10^{-2} at $1.55 \mu\text{m}$ that is two orders of magnitude higher. In this case the corresponding beat length is $145.5 \mu\text{m}$, it is shown in Fig.4 (b). We further study the influence of the air-hole diameter d_2 in the first cladding on the birefringence. Fig.5 (a) shows, when $d_1/\Lambda=0.65$, $\Lambda=1\mu\text{m}$, $\eta_1=2$, $\eta_2=2.4$ and d_2 ranging from 0.65 to 0.85. We can see that the birefringence increases with the increases wavelength and the different air filling fractions d/Λ . These parameters give a value of birefringence 1.68×10^{-2} at $1.55 \mu\text{m}$ is two orders of magnitude higher than that of conventional polarization maintaining fibers and where when $d_2=0.85$, $\lambda > 1.5 \mu\text{m}$, the birefringence instead reduces. It is because the light gradually spread by increased wavelength. In this case the corresponding beat length is $91.85 \mu\text{m}$, it is shown in Fig.5 (b). Compared to these two parameters, the simulation results show that the diameter of the air holes d_2 plays an important role in the birefringence of PCFs.

Then we calculate easily the confinement loss

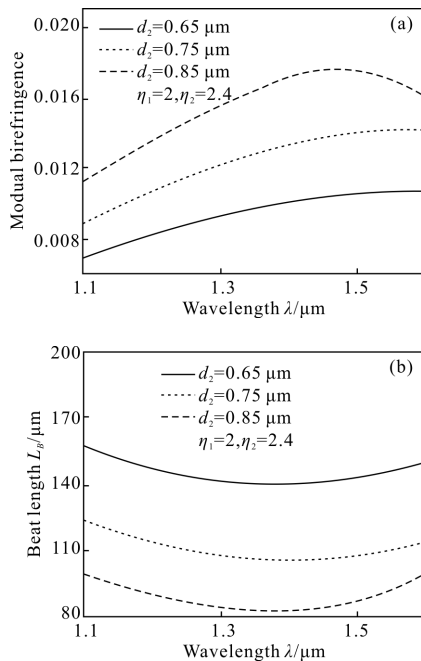


Fig.5 Birefringence and beat length of the structure for the changes d_2

by Eq. (6) for the optimized HB–HN–OPCF, when the pitch $\Lambda=1\mu\text{m}$, elliptical ratio $\eta_1=2$, $\eta_2=2.4$ and air filling ratio are $d_1/\Lambda=0.65$ and $d_2/\Lambda=0.85$ are kept constant. The simulation results are shown in Fig.6. From the Fig.6 (a) we can clearly see, the model confinement loss L_c increases with the increases wavelength, and the confinement loss is less than 10^{-7} dB/km in the wavelength range of $1.2 \mu\text{m}$ to $1.6 \mu\text{m}$. It is found that a very low L_c of the proposed OPCF of 0.6 dB/km at wavelength $1.55 \mu\text{m}$ was obtained. The 2D mode field intensity distribution of the fundamental mode for the OPCFs at wavelength $1.55 \mu\text{m}$ is shown in Fig.6(b). It can be clearly seen the mode field intensity are more strongly confined in the core region and the shape is ellipse that important to get the high birefringence.

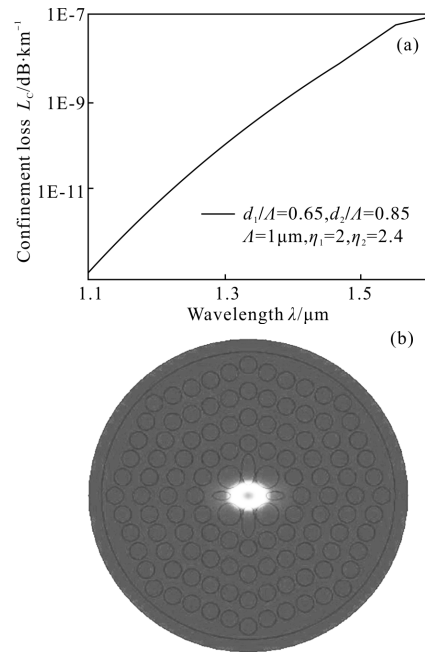


Fig.6 Confinement loss and intensity profile at wavelength $1.55 \mu\text{m}$ of the optimized OPCF

Table1 shows a detailed comparison between properties of the proposed HPCF, SPCF and OPCF, considering the nonlinear coefficient γ value variation and birefringence B of our PCF. The nonlinear coefficients in all reference are not larger enough and it is not match to the high

nonlinearity requirements of optical fiber communication. It should be pointed out that the birefringence is not considered in reference [16–18, 20]. Although, the PCFs in reference [8, 15, 21–25] show, the birefringence is reached to 10^{-3} and higher one order of magnitude than common optical fibers, but it still can not satisfy the need of optical fiber communication and sensing system for better optical fibers with better features, such as high polarization. On the other hand, our proposed PCFs have shown better high nonlinear coefficient and high birefringence at wavelength $1.55 \mu\text{m}$ compared with PCF in Tab.1.

Tab.1 Comparison of nonlinear coefficient and birefringence from different reference at $\lambda=1.55\mu\text{m}$

Type	Nonlinear coefficient/ $\text{W}^{-1}\text{km}^{-1}$	Birefringence/ $(10^{-3}-10^{-2})$
Ref.[8]	19	1.3×10^{-3}
Ref.[15]	20	10^{-4}
Ref.[16]	31.5	–
Ref.[17]	30	–
Ref.[18]	45	–
Ref.[19]	49	1.01×10^{-2}
Ref.[20]	54	–
Ref.[21]	46	3.2×10^{-3}
Ref.[22]	28	2.1×10^{-3}
Ref.[23]	60.5	4.92×10^{-3}
Ref.[24]	42	1.53×10^{-2}
Ref.[25]	41	1.78×10^{-8}
Ref.[26]	10	10^{-3}
Our proposed	60	1.68×10^{-2}

3 Conclusion

We proposed a simple index-guiding OPCF structure in which the elliptical air-holes with elliptical ratio $\eta_1=a_1/b_1$ arranged along x -axis and elliptical ratio $\eta_2=a_2/b_2$ arranged along y -axis are introduced near the core region. The influence of elliptical ratio η_2 and circular air-hole d_2 on the modal nonlinearity, birefringence and confinement

loss are numerically investigated by using finite element method with anisotropic perfectly matched layers. The results are summarized at wavelength $1.55 \mu\text{m}$ that our proposal shows low confinement loss $L_c=0.6 \times 10^{-7} \text{ dB/km}$, a small effective mode area $A_{\text{eff}}=2.16 \mu\text{m}^2$, high nonlinearity $\gamma=60 \text{ W}^{-1}\text{km}^{-1}$ as well as high birefringence $B=1.68 \times 10^{-2}$, and the birefringence is two orders of magnitude higher than that of conventional polarization maintaining fibers. It has also been found that the parameters η_2 and d_2 is particularly important in controlling the nonlinearity, birefringence and confinement loss properties of the OPCF. Compared to the previous study the results of our proposed it is better. This highly birefringence PCFs with high nonlinear coefficient can be used in telecommunication, various polarization sensitive devices and supercontinuum applications systems.

Reference:

- [1] Knight J C, Birks T A, St P J. Russell. All-silica single-mode optical fiber with photonic crystal cladding [J]. *Opt Lett*, 1996, 21(19): 1547–1549.
- [2] Reeves W H, Knight J C, Russell P J St, et al. Demonstration of ultra-flattened dispersion in photonic crystal fibers [J]. *Opt Express*, 2002, 10(14): 609–613.
- [3] Limpert J, Schreiber T, Nolte S, et al. High-power air-clad large-mode-area photonic crystal fiber laser [J]. *Opt Express*, 2003, 11(7): 818–823.
- [4] Ortigosa-Blanch A, Knight J C, Wadsworth W J. Highly birefringent photonic crystal fibers [J]. *Opt Lett*, 2000, 25(18): 1325–1327.
- [5] Yoshinori Namihira, Liu Jingjing. Design of highly nonlinear octagonal photonic crystal fiber with near-zero flattened dispersion at $1.31 \mu\text{m}$ waveband [J]. *Optical Review*, 2011, 18(6): 436–440.
- [6] Chau Y F, Yeh H H, Tsai D P. Significantly enhanced birefringence of photonic crystal fiber using rotational binary unit cell in fiber cladding [J]. *Japanese Journal of Applied Physics*, 2007, 46: L1048.
- [7] Kejalakshmy K, Rahman B M A, Agrawal A, et al. Characterization of single-polarization single-mode photonic crystal fiber using full-vectorial finite

- element [J]. *Method Appl Phys B*, 2008, 93: 223–230.
- [8] Yamamoto T, Kubota H, Kawanishi S, et al. Supercontinuum generation at 1.55 μm in a dispersion-flattened polarization-maintaining crystal fiber [J]. *Opt Express*, 2003, 11(13): 1537–1540.
- [9] Steel K J, Osgood R M. Polarization and dispersion properties of elliptical-hole photonic crystal fiber [J]. *J Lightwave Technol*, 2001, 19(4): 495–503.
- [10] Yue Y, Kai G, Zhi Wang, et al. Highly birefringence elliptical-hole photonic crystal fiber with squeezed hexagonal lattice [J]. *Opt Lett*, 2007, 32(5): 469–471.
- [11] Ortigosa-Blanch A, Díez A, Pinar M D. Ultrahigh birefringent nonlinear microstructured fiber [J]. *IEEE Photon Technol Lett*, 2004, 16(7): 1667–1669.
- [12] Lehtonen M, Genty G, Kaivola M, et al. Supercontinuum generation in a highly birefringence microstructured fiber [J]. *Appl Phys Lett*, 2003, 82(14): 2197–2199.
- [13] Lee J H, Teh P C, Yusoff Z, et al. A holey fiber-based nonlinear thresholding device for optical CDMA receiver performance enhancement [J]. *IEEE Photon Technol Lett*, 2002, 14(6): 876–878.
- [14] Wang Wei, Zhu Zimin. Analysis of photonic crystal fibers and its application in supercontinuum [J]. *Infrared and laser Engineering*, 2007, 36(5): 684–688. (in Chinese)
- [15] Hansen K P, Jensen J R, Jacobsen C. Highly nonlinear photonic crystal fiber with zero-dispersion at 1.55 μm [C]//Optical fiber Communication Conference, 2002: FA9.
- [16] Xu Huizhen, Wu Jian, Xu Kun, et al. Highly nonlinear all-solid photonic crystal fibers with low dispersion slope [J]. *Applied Optics*, 2012, 5(8): 1021–1027.
- [17] Kunimasa Saitoh, Masanori Koshihira. Highly nonlinear dispersion-flattened photonic crystal fibers for supercontinuum generation in a telecommunication window [J]. *Opt Express*, 2004, 12(10): 2027–2032.
- [18] Feroza Beguma, Yoshinori Namihira, Abdur Razzak S M. Design and analysis of novel highly nonlinear photonic crystal fibers with ultra-flattened chromatic dispersion [J]. *Opt Commun*, 2009, 282(7): 1416–1421.
- [19] Ademgil H, Haxha S. Highly nonlinear birefringent photonic crystal fiber [J]. *Opt Commun*, 2009, 282: 2831.
- [20] Feroza Begum, Yoshinori Namihira. Highly nonlinear photonic crystal fibers for supercontinuum generation at 1.06 μm , 1.31 μm and 1.55 μm wavelengths [C]//15th opto electronics and communications conference (OECC2010) technical digest sapporo convention center, Japan 2010: 640–641.
- [21] Zhang Yani. Optimization of highly nonlinear dispersion-flattened photonic crystal fiber for supercontinuum generation [J]. *Chin Phys B*, 2013, 1(22): 014214.
- [22] Xu Qiang, Miao Runcai, Zhang Yani. Highly birefringence low-dispersion of nonlinear photonic crystal fiber [J]. *Optik*, 2012, 124(15): 2269–2272.
- [23] Xu Qiang, Miao Runcai, Zhang Yani. Highly nonlinear low-dispersion photonic crystal fiber with high birefringence for four-wave mixing [J]. *Optical Materials*, 2012, 35: 217–221.
- [24] Abdur Razzak S M, Yoshinori Namihira. Numerical design of high nonlinear coefficient of microstructure optical fibers [J]. *Optik*, 2011, 122(12): 1084–1087.
- [25] Cao Ye, Li RongMin, Tong Zhengrong. Investigation of a new kind of high birefringence photonic crystal fiber [J]. *Acta Phys Sin*, 2013, 62(8): 084215. (in Chinese)
- [26] Wang Wei, Yang Bo. Characteristic analyses of high birefringence and two zero dispersion points photonic crystal fiber with Octagonal lattice [J]. *Acta Phys Sin*, 2012, 61(14): 144601. (in Chinese)
- [27] Chiang J S, Wu T L. Analysis of propagation characteristics for an octagonal photonic crystal fiber (O-PCF) [J]. *Opti Commun*, 2006, 258(2): 170–176.
- [28] Ademgil H, Haxha S. Highly birefringent photonic crystal fibers with ultralow chromatic dispersion and low confinement losses [J]. *J Lightwave Technol*, 2008, 26(4): 441–447.
- [29] Selleri S, Vincetti L. Complex FEM modal solver of optical waveguides with PML boundary conditions [J]. *Opt Quant Electron*, 2001, 33: 359–371.
- [30] Niels Asger Mortensen. Effective area of photonic crystal fibers [J]. *Opt Express*, 2002, 10(7): 341–348.